Upper and Lower Jaramillo polarity transitions recorded in IODP Expedition 303 North Atlantic sediments: Implications for transitional field geometry

A. Mazaud, J.E.T. Channell, C. Xuan, J.S. Stoner

Accepted Manuscript

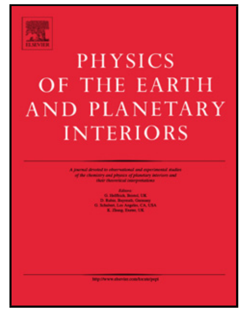

Title: Upper and Lower Jaramillo polarity transitions recorded in IODP Expedition 303 North Atlantic sediments: Implications for transitional field geometry

Authors: A. Mazaud, J.E.T. Channell, C. Xuan, J.S. Stoner

PII:	S0031-9201(08)00223-9
DOI:	doi:10.1016/j.pepi.2008.08.012
Reference:	PEPI 5042
To appear in:	*Physics of the Earth and Planetary Interiors*
Received date:	16-4-2008
Revised date:	5-8-2008
Accepted date:	6-8-2008

Please cite this article as: Mazaud, A., Channell, J.E.T., Xuan, C., Stoner, J.S., Upper and Lower Jaramillo polarity transitions recorded in IODP Expedition 303 North Atlantic sediments: implications for transitional field geometry, *Physics of the Earth and Planetary Interiors* (2007), doi:10.1016/j.pepi.2008.08.012

Upper and Lower Jaramillo polarity transitions recorded in IODP Expedition 303 North Atlantic sediments: implications for transitional field geometry

A. Mazaud[1], J.E.T. Channell[2], C. Xuan[2] and J.S. Stoner[3]

[1] Laboratoire des Sciences du Climat et de l'Environnement, CEA-CNRS, domaine du CNRS, 91198 Gif-sur-Yvette France

[2] Department of Geological Sciences, University of Florida, PO Box 112120, 241 Williamson Hall, Gainesville, FL 32611, USA.

[3] College of Oceanic and Atmospheric Sciences (COAS), Oregon State University 104 COAS Administration Building, Corvallis, OR 97331-5503

Abstract:

Sediments collected during the Integrated Ocean Drilling Program (IODP) Expedition 303 in the North Atlantic provide records of polarity transitions and geomagnetic excursions at a high resolution. Here we investigate polarity transitions at the upper and lower boundaries of the Jaramillo Subchronozone at Sites U1305, U1304, and U1306. The sediments carry strong natural remanent magnetizations (NRM) with median destructive fields consistent with magnetite as the dominant magnetic carrier. Both polarity transitions are characterized by low values of relative paleointensity. The U1305 record of the lower Jaramillo reversal exhibits a marked cluster of virtual geomagnetic poles (VGP) over southern South America, and a secondary accumulation in the region of NE Asia / North Pacific. The main South American VGP cluster is also visible at Site U1304, which documents a less complex pattern, possibly because of a higher degree of smoothing. Records of the upper Jaramillo polarity transition document a VGP loop over the Americas, followed by north to south motion including a secondary VGP accumulation near India. The similarity between several records of the upper Jaramillo transition obtained at various sites in the North Atlantic is a

strong indication that geomagnetic field changes have been faithfully captured. Results suggest that a transverse, possibly dipolar, component has fluctuated during these polarity reversals, and that these fluctuations combined with a reduced axial dipole component yielded the observed field at the Earth's surface during the polarity transitions. The lower Jaramillo transition also exhibits VGP clusters in the vicinity of South America and eastern Asia but these clusters are shifted relative to the upper Jaramillo VGP clusters, implying a memory exerted by the upper mantle on polarity transition geometry.

1 – Introduction

Integrated Ocean Drilling Program (IODP) Expedition 303 was conducted in September-November 2004, with the principal objective of exploring the millennial-scale climate variability in the North Atlantic Ocean during the Quaternary and late Neogene. Such studies require not only adequate sedimentation rates but also a viable means of long-distance stratigraphic correlation at an appropriate resolution. In this respect, paleomagnetic records, particularly records of relative paleointensity, provide the means of augmenting more traditional stable isotope records. In addition, such studies provide information on the high-resolution behavior of the geomagnetic field that can be utilized by geophysicists investigating the geodynamo.

Sediments were obtained using the Advanced Piston Corer (APC), with non-magnetic core barrels which limit magnetic overprint during the coring process [Lund et al., 2003]. Many of the drilled sites are characterized by high mean Quaternary sedimentation rates, of 15 –20 cm/kyr [Channell et al., 2006]. The high sedimentation rates, combined with the fidelity of the natural remanent magnetization (NRM) records, provide the opportunity to study the configuration and paleointensity of the geomagnetic field during polarity reversals. The configuration of the transitional field at polarity reversals remains poorly documented due to the paucity of sedimentary records with sufficient resolution to record these millennial-scale processes, and the intermittent character of volcanic reversal records. Here, we present results obtained at Sites U1304, U1305 and U1306 for the polarity transitions at the top and base of the Jaramillo Subchronozone.

2- Drilling sites and shipboard paleomagnetic results

Sites drilled during the IODP Expedition 303 are described in detail in the IODP Volume 303/306 Expedition Report [Channell et al., 2006]. At Site U1305, located at the southwestern extremity of the Eirik Drift off southern Greenland (Lat 50°10'N, Long 48°31 W), three holes recovered sediments from the Brunhes and Matuyama Chronozones, including the Jaramillo Subchronozone. Water depth at this site is 3460 m (Fig. 1) such that the sediment-water interface is located below the present-day main axis of the Western Boundary Undercurent (WBUC). For this reason, and on the basis of oxygen isotope stratigraphies from neighboring sites documenting the last glacial cycle, the site is likely to be characterized by expanded interglacials and relatively condensed glacial stages. The base of the section lies within the Olduvai Subchronozone at about 1.8 Ma with a mean sedimentation rate of 17 cm/ kyr [Shipboard Scientific Party, 2006]. Sediments recovered at the site comprise silty clays with nannofossils. Paleomagnetic measurements were conducted shipboard on archive half core sections comprised measurements of NRM using the shipboard pass-through cryogenic magnetometer. The spatial resolution of the shipboard magnetometer, as measured by the width at half-height of the pickup coil response function, is about 10 cm for each of the three orthogonal axes. Aboard ship, NRM intensity and direction of half-core sections were measured before any demagnetization, and re-measured after limited alternating field (AF) demagnetization, restricted to peak fields of 10 mT, or occasionally 20 mT. Low peak demagnetization fields ensure that archive halves remain useful for shore-based high-resolution measurements of u-channel samples. NRM intensities before demagnetization range from $\approx 10^{-1}$ to more than 1 A/m. After AF demagnetization at peak fields of 10-20 mT, intensities are reduced to $\approx 10^{-1}$ A/m. NRM inclinations vary around the value expected for a geocentric axial dipole, for both normal and reverse polarity intervals. Despite the limited AF demagnetization, the Brunhes and the upper Matuyama subchronozones were clearly identified in shipboard records [Shipboard Scientific Party, 2006].

Site U1306 (Lat 58°14’N, Long 45°38’W) was drilled South of Greenland, in a water depth of ≈ 2270 m in the main axis of the Western Boundary Undercurent (WBUC). Sediments comprise silty clays with varying amounts of diatoms, nannofossils and foraminifera [Shipboard Scientific Party, 2006]. Based on stratigraphies for the last glacial cycle obtained from conventional piston cores in the region, we expect glacial intervals to be expanded relative to interglacials, providing a stratigraphy that is complementary to that obtained at Site U1305. Shipboard paleomagnetic measurements revealed NRM intensities prior to demagnetization in the 10^{-1} A/m range. After AF demagnetization at peak fields of 10 or 20 mT, NRM intensities were reduced by about 50%. Inclinations vary around the expected values for a geocentric axial dipole for normal and reverse polarity intervals. The Brunhes Chronozone and the upper Matuyama subchronozones were clearly identified from shipboard magnetic measurements [Shipboard Scientific Party, 2006].

Site U1304 (Lat 53°03’N, Long 33°32 W) was drilled at the southern edge of the Gardar Drift in a water depth of ≈ 3065 m. The objective was to compare climatic and paleomagnetic records to those previously obtained on the northern part of the Gardar Drift during ODP Leg 162 (Site 983). Sediments at Site U1304 comprise interbedded diatom oozes and nanofossil ooze with intervals of clay and silty clay. Shipboard paleomagnetic measurements document NRM intensity in the range of 10^{-1} A/m for most intervals. Intervals rich in diatom oozes are less strongly magnetized with intensities in the range of 10^{-3} A/m. An almost continuous sequence was obtained including the Brunhes Chron and part of the Matuyama Chron, including the Jaramillo and Cobb Mountain Subchronozones, and the top of the Olduvai Subchronozone [Shipboard Scientific Party, 2006].

3 Sampling and laboratory methods

Core sections from IODP Sites U1304, U1305 and U1306 recording geomagnetic polarity transitions and excursions were sampled with u-channels at the IODP core depository in Bremen (Germany) in February 2005 prior to the main sampling in May 2005. The objective was to measure polarity transitions in u-channels from the working halves of core sections that would later be sub-sampled for other purposes during the main sampling party three months later. Natural remanent magnetization (NRM) and bulk magnetic parameters were measured at a high-resolution with pass-through cryogenic magnetometers designed for long-core measurements [Weeks et al., 1993] at the LSCE in Gif-sur-Yvette (France) and at the University of Florida, Gainesville. Stepwise AF demagnetization of the NRM was conducted up to peak fields of 100 mT using the in-line 3-axes AF coils system. Component magnetization directions were then determined for the 20-60, or 20-80 mT demagnetization interval using the standard "principal component" method of Kirschvink (1980) either through the standard software used at the University of Florida, or through the Excel routine used at Gif-sur-Yvette [Mazaud et al., 2005]. Declinations of the resolved component magnetizations were adjusted according to the shipboard "Tensor Multishot" orientation tool when available, or by uniform rotation of cores such that the core mean declinations for intervals outside the polarity transitions equaled 0° or 180°, depending on the sign of the inclination.

After measurement of NRM, the following magnetic concentration parameters were measured on all u-channels: volume low-field susceptibility (κ), anhysteretic remanent magnetization (ARM), and the isothermal remanent magnetization (IRM). κ is controlled by the amount, nature and grain size of ferromagnetic (s.l.) and is also inluenced by paramagnetic and diamagnetic minerals. ARM and IRM, on the other hand, are remanent magnetizations, and therefore solely sensitive to the ferromagnetic (s.l.) fraction, and do not depend on paramagnetic minerals. ARM is principally linked to small magnetic grains, with size around 0.1 – 5 µm, while IRM is sensitive to a wider spectrum of grain sizes up to several tens of microns [Maher, 1988; Dunlop and Ozedemir, 1997]. ARM was acquired along the axis of the u-channel using a 100 mT AF field and a 50 µT DC field. It was demagnetized using the same steps than those used for the NRM. IRM was acquired in 6 steps up to 1 T using a 2G pulsed IRM solenoid. IRM_{1T} was stepwise demagnetized. Then, after a re-acquisition at 1 T, a backfield of 0.3 T was applied to calculate the S-ratios$_{-0.3T}$ ($S_{-0.3T}$. = -$IRM_{-0.3T}$./IRM_{1T}. [King and Channell, 1991]), which provides a measure of magnetic coercivity spectrum that can also be gauged by hysteresis experiments conducted with a Princeton Measurements Corp. alternating gradient magnetometer (AGM) or vibrating sample magnetometer (VSM). Measurements of the low field bulk susceptibility (κ) were performed using a small diameter Bartington sensor loop mounted in line with a track system designed for u-channels at Gif-sur-Yvette and a Sapphire loop with susceptibility track designed for u-channels at the University of Florida [Thomas et al., 2003].

4. Records of polarity transitions

4.1 Lower Jaramillo transition

The lower Jaramillo polarity transition is recorded in the composite section at Site U1305 [Shipboard Scientific Party, 2006] between 167 and 169 meters composite depth (mcd). Orthogonal projections of AF demagnetization data indicate progressive decrease of NRM intensity at peak fields greater than 20 mT (Fig. 2a). Component magnetization directions were calculated for the 20 to 60 mT AF peak field interval (Fig. 2b and 2c) Maximum angular deviations (MAD) values [Kirschvink, 1980] (Fig. 2d) indicate the precision of the definition of magnetization components. Median destruction fields of about 27 mT is obtained for ARM, which is consistent with magnetite or low Ti (titano)magnetite as the dominant carrier of the NRM. NRM/ARM is a proxy commonly used for relative paleointensity determinations [Banerjee and Mellema, 1974; Levi and Banerjee, 1976; King et al., 1983; Tauxe, 1993]. Here we used the NRM-ARM slope calculated in the 20-60 mT AF peak field range [Channell et al., 2002]. The linear correlation coefficient (r) indicates well-defined slopes with values around 0.99 outside the transition and higher than 0.95 during the reversal (Fig. 2i). The NRM/ARM slopes indicate a broad low at the time of directional changes associated with the polarity transition. Interestingly, the paleointensity was significantly reduced prior the directional reversal (Fig. 2i). Virtual geomagnetic poles (VGPs) were then calculated from the NRM component directions. The plot of VGPs (Fig. 2g) is used here as a convenient means of documenting directional changes at the reversal (in addition to Figs. 2 b-d), and does not imply that the transitional fields were dipolar. VGP latitudes fluctuate prior the transition in the 168.5-169.6 mcd interval (Fig. 2h), however, these fluctuations occur in an interval where the bulk magnetic parameters (κ, ARM, IRM and ARM/ κ) also fluctuate around relatively high values (Fig. 2e). The polarity transition onset at about 168 mcd is marked by an accumulation of VGPs over the South America. The VGP then moves to the northern hemisphere, with a large longitudinal drift and a secondary accumulation of VGPs over eastern Asia (Fig. 2g).

Another record of the same transition was obtained at Hole U1304B at ≈ 176 mcd (Fig. 3). Stable magnetization components were isolated after AF demagnetization at peak fields of ≈ 20 mT (as before component magnetization directions were calculated in the 20-60 mT peak field range). Bulk magnetic parameters display very limited variations, indicating that, in this case, the paleomagnetic record is not strongly perturbed by changes in concentration and grain size of the magnetic fraction. A broad low in relative paleointensity

(NRM-ARM slope) coincides with the directional transition (Fig. 3i). No fluctuations are observed prior the transition. However, only a limited interval prior to the transition was sampled. This VGP path shows a less complex pattern than at site U1305. This could be due to more smoothing of the transition record at Site U1304 than at Site U1305. A VGP cluster near southern America is apparent at the onset of the polarity transition. The VGP motion to the northern hemisphere resembles that obtained at Site U1305. No longitudinal drift of the VGP is visible in the last part of this record of the lower Jaramillo transition.

4.2. Upper Jaramillo transition

This polarity transition is recorded between ≈ 156 and 158 mcd at Hole U1305A (Fig. 4). AF demagnetization indicates that a stable magnetization component is resolved after ≈ 20 mT peak field demagnetization. As for the other transitions, the characteristic NRM directions were calculated for the 20-60 mT peak field range, and MAD values were calculated. Fluctuations of the bulk magnetic parameters are very limited in the vicinity of the transition, suggesting that magnetic concentration and grain size were more uniform for the upper Jaramillo transition than for the lower Jaramillo transition at Site U1305. NRM-ARM slopes are well defined (Fig. 4i) and they indicate reduced field intensity at the time of directional changes. VGP motion starts from the North pole with a large loop over the Americas, followed by a progressive move from the North pole to the South pole that includes a secondary accumulation of VGPs at low latitudes in the Indian Ocean. A short post-transitional excursion is observed at ≈155.5 mcd (Fig. 4).

Record obtained at Hole U1306D (Fig. 5) offers a very detailed view of the same transition trajectory, with a transitional zone over more than 2 m. As for Hole 1305A, stable component was isolated after 20mT peak alternating field demagnetization. Characteristic NRM directions were calculated for the 20 - 80 mT peak field range, and are clearly defined through the entire transitional zone. NRM-ARM slopes indicate a broad low in relative paleointensity which coincides with the directional reversal (Fig. 5). Magnetite abundance and grain size proxies document limited variability and do not correlate with characteristic NRM directions or intensity changes (Fig. 5). Overall, the VGP trajectory calculated from the characteristic directions (Fig. 5) is very similar to that of Site U1305, with a large VGP swing over the Americas prior a pole-to-pole transition showing a secondary cluster (Fig 5).

Finally, another record of the Upper Jaramillo transition was obtained at Hole U1304B in the 164 and 165 mcd interval (only a limited interval around this transition was sampled). ARM, IRM, □ and ARM/□ (Fig. 6) indicate homogeneity in amount and size of magnetite grains. The VGP path calculated from the characteristic NRM directions is less complex than at Sites U1305 and U1306 (Fig 6), presumably because of a higher smoothing of the polarity transition at this site. Nevertheless, a strong resemblance with the records from sites U1305-U1306 records is observed. Records at sites U1305 and U1306 are remarkably similar to the record previously obtained at ODP Site 983 (ODP Leg 162) [Channell and Lehman, 1997] (Fig. 7). Overall, the similarity between several records obtained at various sites in the North Atlantic is a strong indication that geomagnetic field changes during this transition were correctly captured.

5- Discussion and conclusion

Detailed records obtained for the upper and lower Jaramillo polarity transitions from IODP Expedition 303 sediments yield VGP trajectories (Fig. 7) that show clusters and loops alternating with fast changes, reminiscent of reversal records previously obtained at ODP Sites 983 and 984, and also of some volcanic records [Channell and Lehman, 1997; Mazaud and Channell, 1999, Channell et al., 2004; Prévot et al., 1985; Mankinen et al., 1985]. The VGP paths do not pass close to the sites or to their antipodes, confirming the idea that the transitional fields are not axi-symmetric. Clusters and loops tend to be located in the two longitudinal bands, one over eastern Asia and another over the Americas, that were recognized over 15 years ago in sedimentary and volcanic records and interpreted to indicate lower mantle influence on transition field geometry [Clement, 1991; Laj et al., 1991; Hoffman, 1992; Love, 1998]. Other causes linked to sedimentary magnetization acquisition rather than to geomagnetic field behavior have been also envisaged for these two bands [Quidelleur et al., 1995]. Such artifacts, however, are hardly compatible with the complex patterns obtained here. In the higher resolution (higher sedimentation rate) records illustrated here, VGPs appear to jump from one longitudinal band to the other during an individual polarity transition.

The similarity between the different records of the upper Jaramillo transition obtained at North Atlantic sites (ODP Sites 983 and 984, and IODP Expedition –303) is a convincing indication that geomagnetic field changes were faithfully captured at these sites (Fig. 7). Transitional VGPs obtained for the upper Jaramillo transition tend to be located in the two preferred longitudinal bands, with a VGP loop over the Americas prior an eastern Asia VGP path with a secondary VGP accumulation, and, finally, in some records, a VGP loop in the vicinity of Australia (Fig. 7). The results suggest a simple mechanism, in which a transverse field, possibly dipolar, has oscillated while the axial dipole was reduced in intensity. In this scheme, the transverse component and a residual axial dipole alternatively dominate the field during the transition. When the intensity of the transversal component is strong, then VGP departs from the pole and moves towards low latitudes. When the transverse component is weak, then VGP moves back towards the north, or south, geographic pole, because of the dominance of the axial dipole term. The initial excursion visible in the upper Jaramillo transition records is consistent with a transversal field growing and then decaying in intensity, while the residual axial dipole does not strongly change. After this loop, the VGPs move to a final reverse polarity along a longitudinal path approximately antipodal to the initial loop (Fig. 7). A transversal field opposed to that responsible for the initial loop may explain this feature, suggesting an oscillation between two opposite configurations. This simple scheme is somewhat reminiscent of the field evolution during geomagnetic excursions, for which an important role for a transversal dipole field has been proposed [Laj et al., 2006; Laj and Channell, 2007]. A model relating VGP path longitude, site location, and motion of magnetic flux patches at the core surface has been proposed [Gubbins and Love, 1998]. A western VGP path (i.e. near the Americas) is expected for a N-R reversals recorded in the north Atlantic, when a pole-wards motion is hypothesized for the flux patches [Gubbins and Love, 1998]. The initial loop over or near the Americas for the upper Jaramillo polarity transition may fit this scheme. During this loop, VGP departure from the North pole and subsequent return to the same pole occurred along almost identical longitudes (Fig. 7), which suggests a reversible evolution of the geomagnetic field, and therefore of the flux patches in the scheme of Gubbins and Love [1998]. Another configuration, however, has to be envisaged for the final VGP motion to the South pole, which occurred at a longitude approximately antipodal to that of the initial loop (Fig. 7). The lack of a precise age model does not allow investigation of the tempo of the geomagnetic field changes during the Jaramillo polarity transitions. At Site U1305, it is observed that the extremity of the initial loop and the secondary VGP accumulation in the final motion to the South pole over Indian Ocean are separated by about 20 cm in the sediment record (Fig. 4). This interval corresponds to about 1 kyr, assuming that the overall mean sedimentation rate at this site can be applied to this interval. This is of the order of theoretical estimates [Hulot and Le Mouël, 1994] for transverse dipole fluctuations in the modern field. At ODP Sites 983 and 984, the records of polarity transitions for the upper Olduvai [Mazaud and Channell, 1999] and for the Brunhes-Matuyama boundary and Jaramillo reversals [Channell and Lehman, 1997; Channell et al., 2004] also exhibits a VGP loops that feature south American and east Asian VGP clusters that suggest a similarity between these two successive reversals implying a memory for the transition field geometry imparted by the influence of the lower mantle. The importance of heat flux across the core-mantle (C-M) boundary in controlling reversal rates in numerical models [Glatzmeier et al., 1999], implies that the C-M heat flux is an important control on transition field geometry. Progressively, high-resolution sedimentary and volcanic records of polarity transitions are converging towards a consistent picture of the geomagnetic field evolution during polarity transitions.

Acknowledgments:

Laboratory investigations have been funded by the French Commissariat à l'Energie Atomique (CEA) and the Centre National de la Recherche Scientifique (CNRS). Participation to the IODP leg 303 was founded by the Integrated Ocean Drilling Program. Alain Mazaud thanks V. Scao for his help with measurements at the LSCE. LSCE contribution n° XXX.

References:

Banerjee, S.K. and Mellema,, J.P., 1974. A new method for the determination of paleointensity from the ARM properties of rocks. Earth Planet Sci. Letters, 23, 177-184.

Channell, J. E. T., and Lehman, B., 1997. The last two geomagnetic polarity reversals recorded in high-deposition rate sediment drifts, Nature, 389, 712-715.

Channell, J. E. T., Mazaud A., Sullivan, P., Turner, S., Raymo, M. E., 2002. Geomagnetic excursions and paleointensities in the 0.9-2.15 Ma interval of the Matuyama chron at ODP Site 983 and 984 (Iceland Basin), J. of Geophysical Reasearch, 107, doi:10.1029/2001JB000491.

Channell, J.E.T., Curtis , J.H., and Flower B.P., 2004. The Matuyama-Brunhes boundary interval (500-900 ka) in North Atlantic drift sediments. Geophys. J. Int., 158, 489-505.

Channell, J.E.T., Kanamatsu, T., Sato, T., Stein, R., Alvarez Zarikian, C.A., Malone, M.J., and the Expedition 303/306 Scientists, 2006. Proc. IODP, 303/306: College Station TX (Integrated Ocean Drilling Program Management International, Inc.). doi:10.2204/iodp.proc.303306.104 .2006.

Dunlop, D. and Özdemir, Ö., 1997. “Rock Magnetism: Fundamentals and Frontiers”, Series: Cambridge Studies in Magnetism (No. 3), Cambridge university press, 595 p.

Glatzmaier, G.A., Coe, R., Hongre, L., and Roberts, P.H., 1999. The role of the Earth’s mantle in controlling the frequency of geomagnetic reversals, Nature, 401, 885-890.

Gubbins D. and Love, J.J., 1998. Preferred VGP paths during geomagnetic polarity reversals: symmetry considerations, Geophys. Res. Lett. 25 n°7, 1079-1082

Hoffman, K. A., 1992. Dipolar reversal states of the geomagnetic field and core-mantle dynamics, Nature, 359, 789-794.

Hulot, G. and Le Mouël, J.L., 1994. A statistical approach to the main magnetic field, Phys. Earth Planet. Inter. 82, 167-183.

King, J.W. and. Channell, J.E.T., 1991. Sedimentary magnetism, environmental magnetism, and magnetostratigraphy, in *US National report to International Union of Geodesy and Geophysics*, Rev. Geophys. Suppl. 358-370.

King, J.W., Banerjee, S.K. and Marvin, J., 1983. A new rock-magnetic approach to selecting sediments for geomagnetic paleointensity studies: application to paleointensity for the last 4000 years. J. Geophys. Res. 88, 5911-5921.

Kirschvink, J. L., 1980. The least square lines and plane analysis of palaeomagnetic data, J.R. Astron. Soc., 62, 319-354.

Laj, C., Mazaud, A., Weeks, R., Fuller, M., Herrero-Bervera, E., 1991. Geomagnetic reversal paths, Nature, 351, 447.

Laj, C. and Kissel, C. Roberts, A, 2006. Geomagnetic field behavior during the Icelandic Basin and Laschamp geomagnetic excursions: A simple transitional field geometry?,Geochem. Geophys. Geosyst. Q03004: doi: 10.1029/2005GC001122.

Laj C., Channell J.E.T., 2007. Geomagnetic Excursions, in: Treatise in Geophysics, Elsevier, G. Schubert Ed. Vol. 5, 373-416.

Levi, S. and. Banerjee, S.K., 1976 On the possibility of obtaining relative paleointensities from lake sediments. Earth Planet. Sci. Letters, 29, 219-226.

Love, J.J., 1998. Paleomagnetic volcanic data and geometric regularity of reversals and excursions, J. Geophys. Res. Vol. 103,12435-12452.

Lund, S.P., Stoner, J.S., Mix, A.C., Tiedermann, R., Blum, P., and the 202 Leg Shipboard Scientific Party , 2003. Proceedings of the Ocean Drilling Program, Initial Reports, Vol. 202.

Maher, B.A., 1988. Magnetic-properties of some synthetic sub-micron magnetites, Geophysical Journal-Oxford, 94(1): 83-96.

Mankinen, E.A., Prévot, M., Grommé, C.S., and Coe, R.S., 1985. The Steens Mountain (Oregon) geomagnetic polarity transition, 1. Directional history, duration of episodes, and rock magnetism: Journal of Geophysical Research, v. 90, p. 10,393-10,416.

Mazaud, A. and Channell, J.E.T., 1999. The top Olduvai polarity transition at ODP Site 983 (Iceland Basin), Earth Planet. Sci. Lett. 166, 1-13.

Mazaud, A., 2005. User-friendly software for vector analysis of the magnetization of long sediment cores, Geochem. Geophys. Geosyst., doi:10.1029/2005GC001036.

Prévot, M., Mankinen, E.A., Grommé, C.S., and Coe, R., 1985. How the geomagnetic field vector reverses polarity, Nature, 316, 230-234.

Quidelleur, X., Holt, J., and Valet J.P.,1995, Confounding influence of magnetic fabric on sedimentary records of a field reversal, Nature, 274, 246-249.

Shipboard Scientific Party. In: Channell, J.E.T., Kanamatsu, T., Sato, T., Stein, R., Alvarez Zarikian, C.A., Malone, M.J., and the Expedition 303/306 Scientists. Proc. IODP, 303/306: College Station TX (Integrated Ocean Drilling Program Management International, Inc.), 2006. doi:10.2204/iodp.proc.303306.104.

Tauxe, L., 1993. Sedimentary records of relative paleointensity of the geomagnetic field: theory and practice, Rev. Geophys., 31, 319-354.

Thomas, R., Guyodo, Y., and Channell, J.E.T., 2003. U-channel track for susceptibility measurements, Geochemistry, Geophysics and Geosystems (G3), 1050, doi: 10.1029/2002GC000454.

Weeks, R. J., Laj, C., Endignoux, L., Fuller, M., Roberts, A.P., Manganne, R., Blanchard, E., Goree, W., 1993. Improvements in long-core measurements techniques: applications in paleomagnetism and palaeoceanography, Geophys. J. Int., 114, 651-662.

Figures:

Figure 1. Location of IODP Sites U1304, U1305 and U1306 in the North Atlantic.

Figure 2. Results obtained for the Lower Jaramillo transition at Hole U1305A a) Typical diagrams of AF demagnetization (Orthogonal projection, open and full circles: inclination, and declination, axes unit: 10^{-6} A/m; some AF demag levels are also indicated along the graphs), b) ChRM declination, c) ChRM inclination, d) MAD, e) ARM and κ, (left scale) and IRM (right scale), f) ARM/k, g) VGP plot (Hammer-Aitoff projection); in gray pre-transitional fluctuations for which a geomagnetic origin is uncertain, see text, h) VGP latitude, i) NRM versus ARM regression values. In the different diagrams, mcd means meters below seafloor.

Figure 3. Results obtained for the Lower Jaramillo transition at Hole U1304B (see Fig. 2 for caption details

Figure 4. Results obtained for the Upper Jaramillo transition at Hole U1305A (see Fig. 2 for caption details)

Figure 5. Results obtained for the Upper Jaramillo transition at Hole U1306D (see Fig. 2 for caption details)

Figure 6. Results obtained for the Upper Jaramillo transition at Hole U1304B (see Fig. 2 for caption details)

Figure 7. Summary of the detailed VGP paths obtained for the Upper and Lower Jaramillo transitions. Records of the Upper Jaramillo and Upper Olduvai transitions previously obtained at site 983 (ODP-162) are also shown [Channell and Lehman, 1997; Mazaud and Channell, 1999]. Orange circles indicate VGP loops and accumulations.

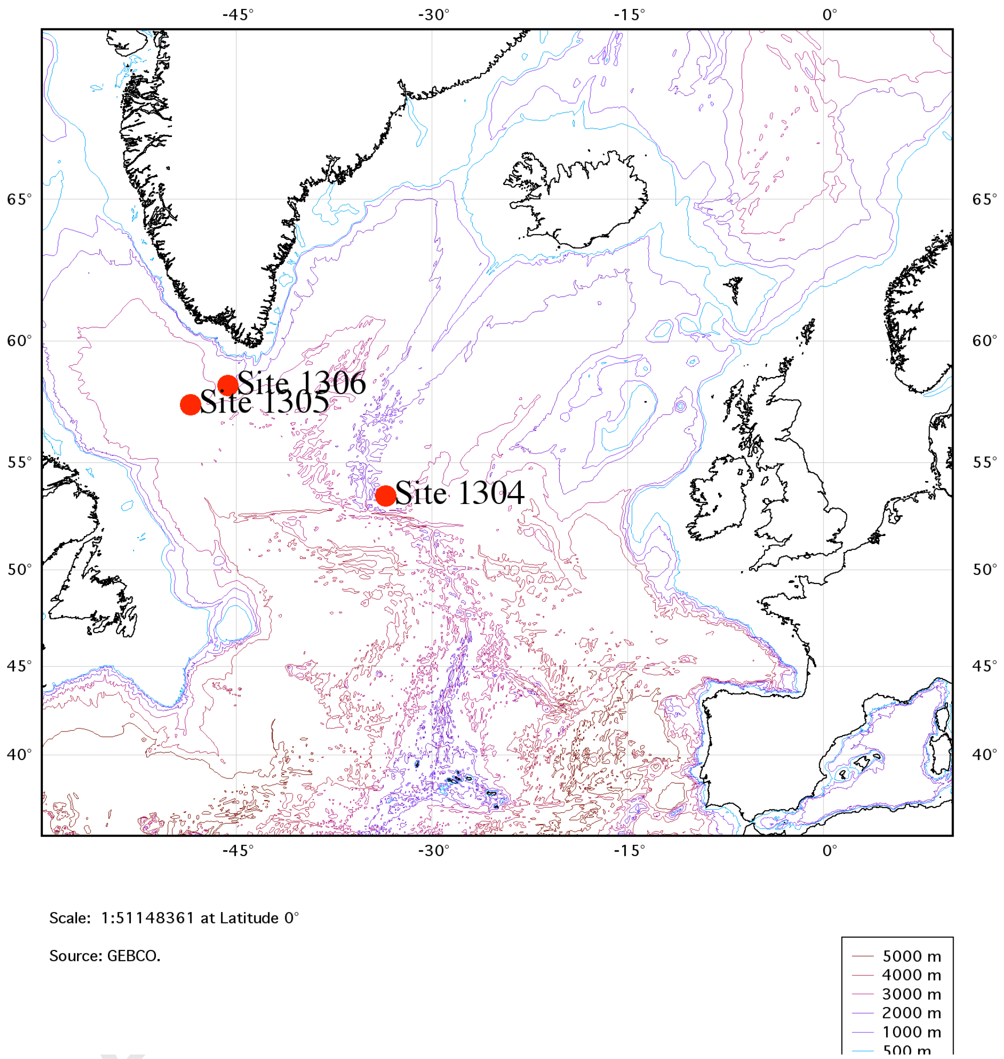

-45°
-30°
-15°
0°
65°
60°
55°
50°
45°
40°
Site 1306
Site 1305
Site 1304
Scale: 1:51148361 at Latitude 0°
Source: GEBCO.
5000 m
4000 m
3000 m
2000 m
1000 m
500 m

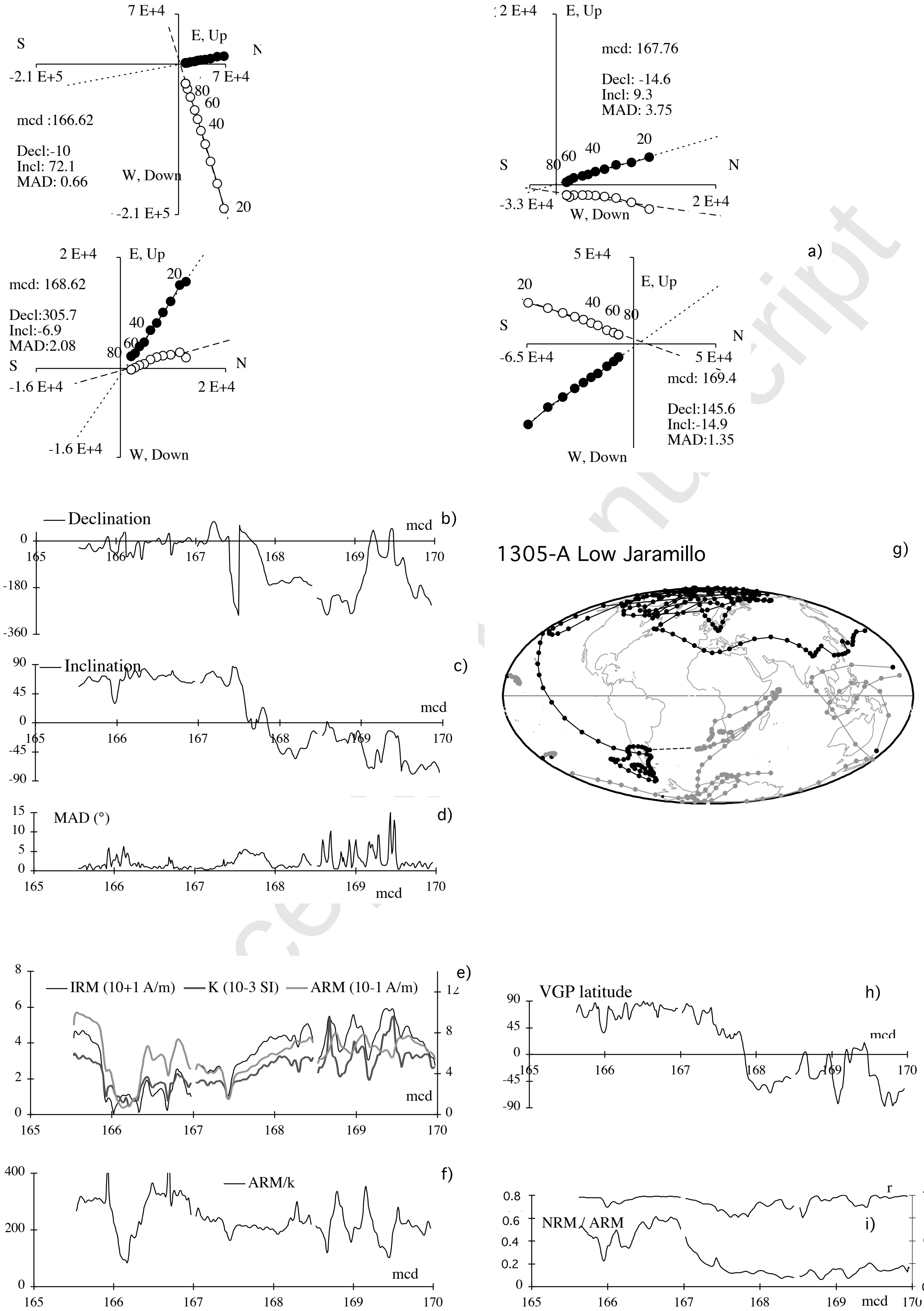
a)
mcd :166.62
Decl:-10
Incl: 72.1
MAD: 0.66
mcd: 167.76
Decl: -14.6
Incl: 9.3
MAD: 3.75
mcd: 168.62
Decl:305.7
Incl:-6.9
MAD:2.08
mcd: 169.4
Decl:145.6
Incl:-14.9
MAD:1.35
E, Up
W, Down
S
N
b)
Declination
c)
Inclination
d)
MAD (°)
e)
IRM (10+1 A/m)
K (10-3 SI)
ARM (10-1 A/m)
f)
ARM/k
g)
1305-A Low Jaramillo
h)
VGP latitude
i)
NRM / ARM
r
mcd

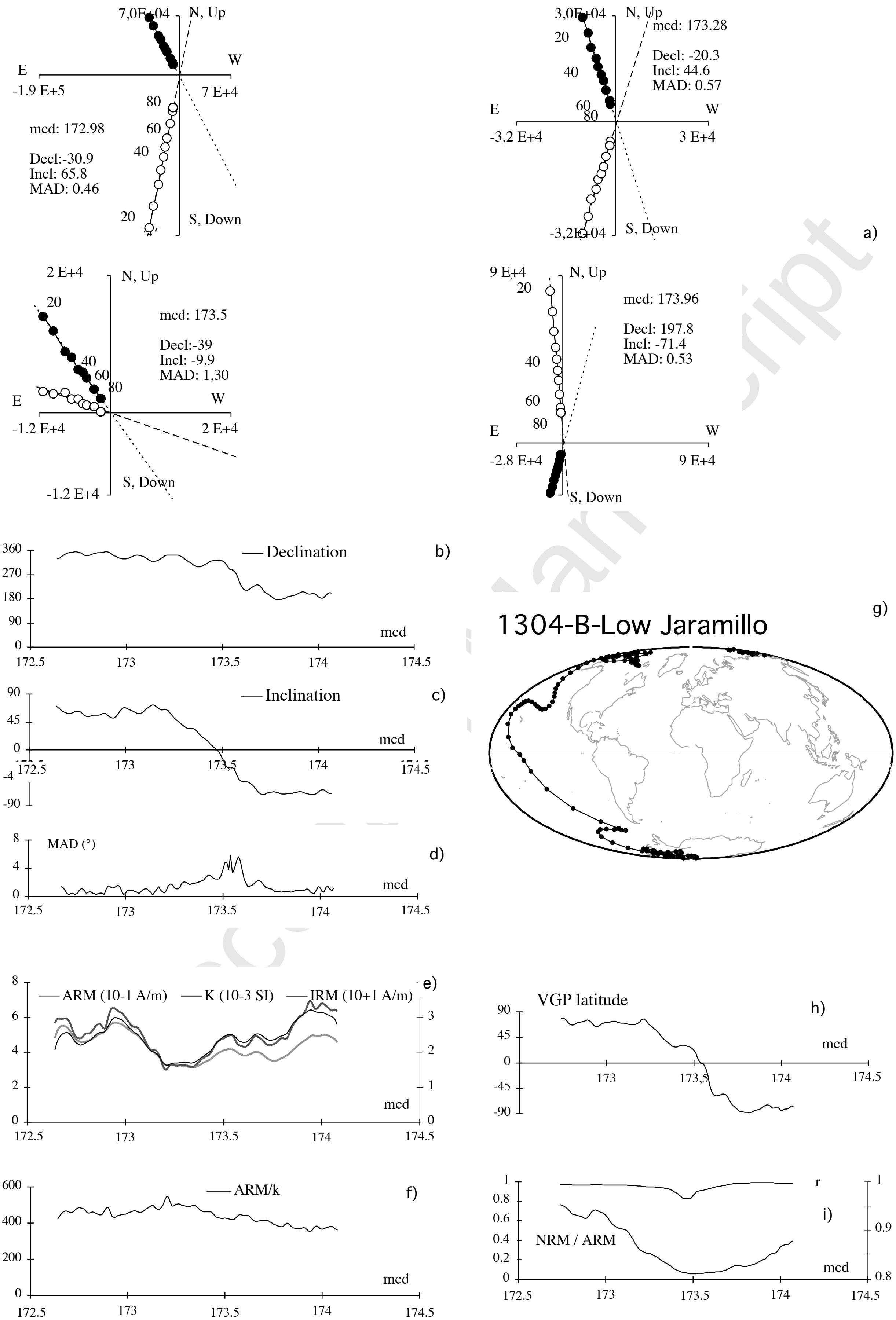
a)
N, Up
S, Down
E
W
7,0E+04
-1.9 E+5
7 E+4
mcd: 172.98
Decl:-30.9
Incl: 65.8
MAD: 0.46
3,0E+04
-3.2 E+4
3 E+4
-3,2E+04
mcd: 173.28
Decl: -20.3
Incl: 44.6
MAD: 0.57
2 E+4
-1.2 E+4
2 E+4
-1.2 E+4
mcd: 173.5
Decl:-39
Incl: -9.9
MAD: 1,30
9 E+4
-2.8 E+4
9 E+4
mcd: 173.96
Decl: 197.8
Incl: -71.4
MAD: 0.53
b)
Declination
c)
Inclination
d)
MAD (°)
mcd
e)
ARM (10-1 A/m)
K (10-3 SI)
IRM (10+1 A/m)
f)
ARM/k
g)
1304-B-Low Jaramillo
h)
VGP latitude
i)
r
NRM / ARM

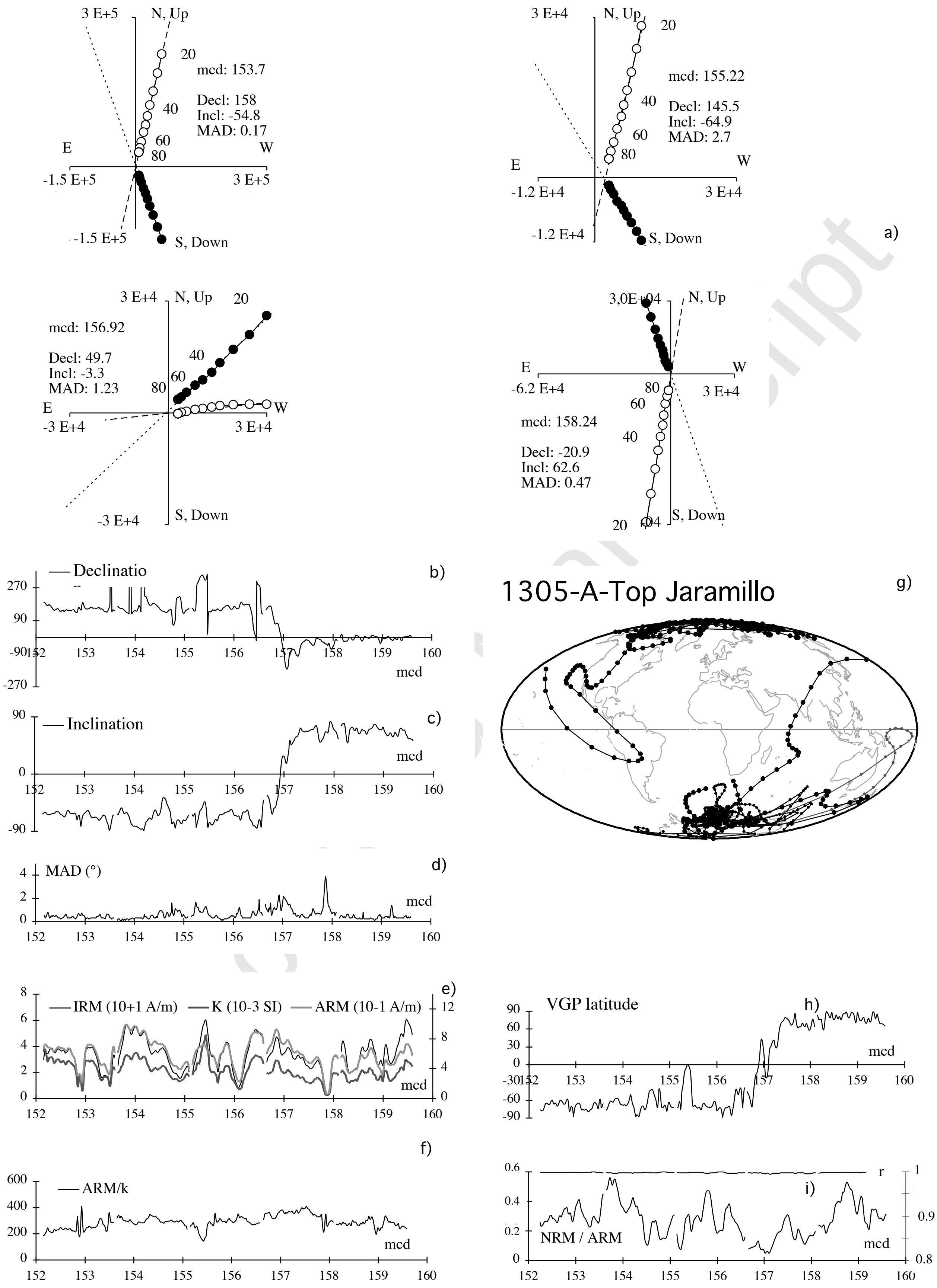
a)
mcd: 153.7
Decl: 158
Incl: -54.8
MAD: 0.17
mcd: 155.22
Decl: 145.5
Incl: -64.9
MAD: 2.7
mcd: 156.92
Decl: 49.7
Incl: -3.3
MAD: 1.23
mcd: 158.24
Decl: -20.9
Incl: 62.6
MAD: 0.47
N, Up
S, Down
E
W
b)
Declinatio
c)
Inclination
d)
MAD (°)
e)
IRM (10+1 A/m)
K (10-3 SI)
ARM (10-1 A/m)
f)
ARM/k
g)
1305-A-Top Jaramillo
h)
VGP latitude
i)
NRM / ARM
r
mcd

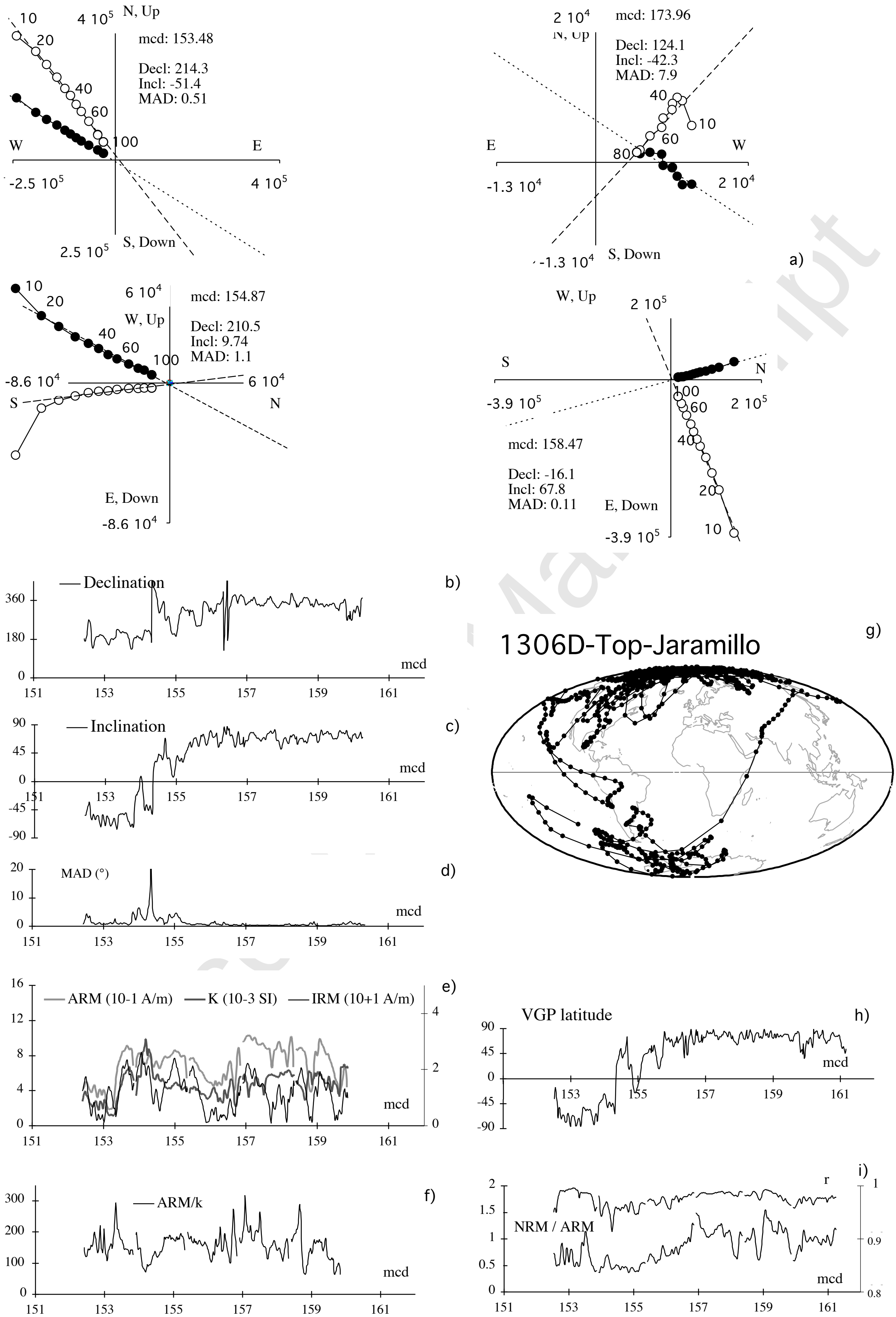
mcd: 153.48
Decl: 214.3
Incl: -51.4
MAD: 0.51
mcd: 173.96
Decl: 124.1
Incl: -42.3
MAD: 7.9
a)
mcd: 154.87
Decl: 210.5
Incl: 9.74
MAD: 1.1
mcd: 158.47
Decl: -16.1
Incl: 67.8
MAD: 0.11
b)
Declination
c)
Inclination
d)
MAD (°)
e)
ARM (10-1 A/m)
K (10-3 SI)
IRM (10+1 A/m)
f)
ARM/k
g)
1306D-Top-Jaramillo
h)
VGP latitude
i)
NRM / ARM
r
mcd

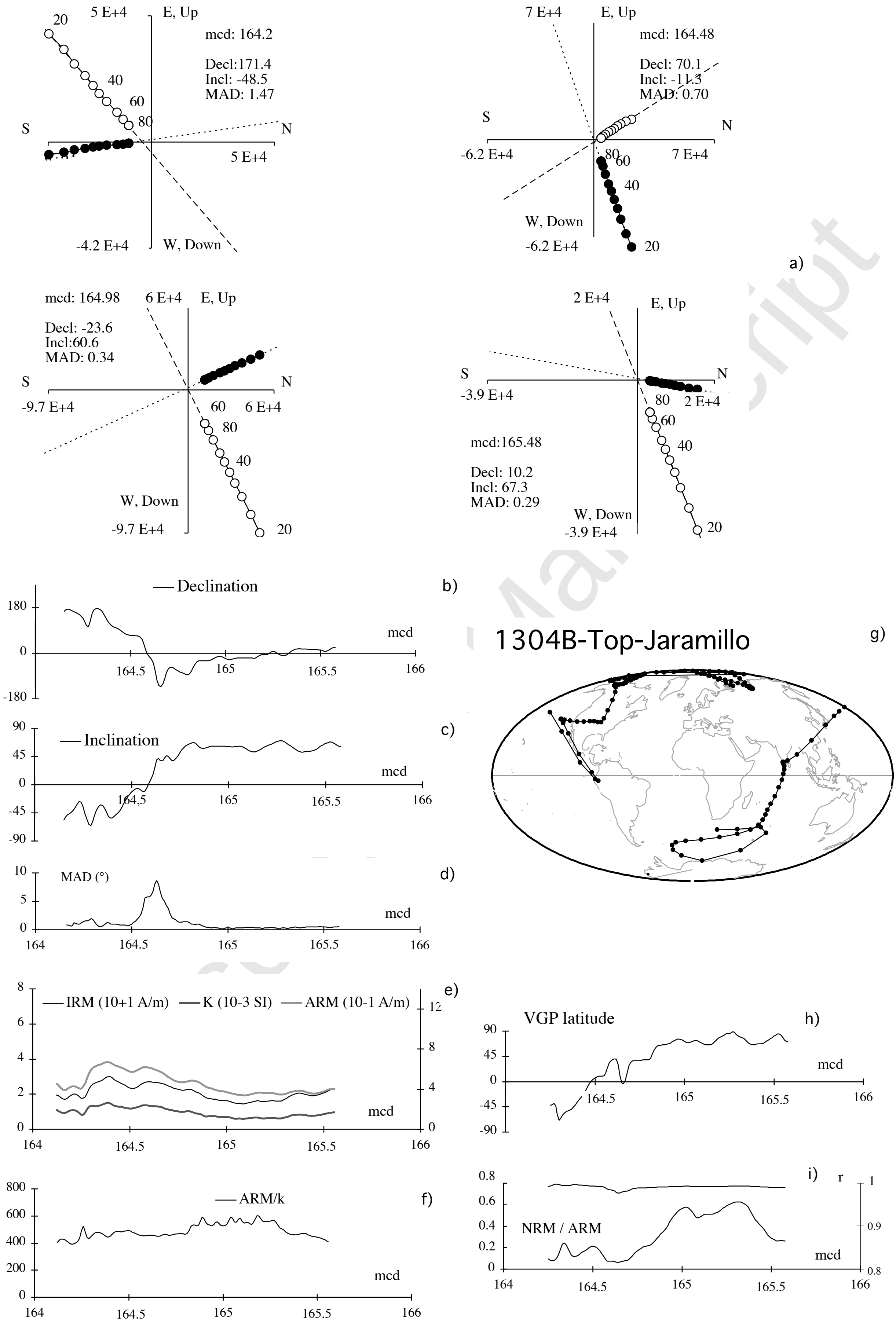

mcd: 164.2
Decl:171.4
Incl: -48.5
MAD: 1.47
mcd: 164.48
Decl: 70.1
Incl: -11.3
MAD: 0.70
a)
mcd: 164.98
Decl: -23.6
Incl:60.6
MAD: 0.34
mcd:165.48
Decl: 10.2
Incl: 67.3
MAD: 0.29
E, Up
W, Down
S
N
Declination
b)
Inclination
c)
MAD (°)
d)
IRM (10+1 A/m)
K (10-3 SI)
ARM (10-1 A/m)
e)
ARM/k
f)
1304B-Top-Jaramillo
g)
VGP latitude
h)
NRM / ARM
r
i)
mcd

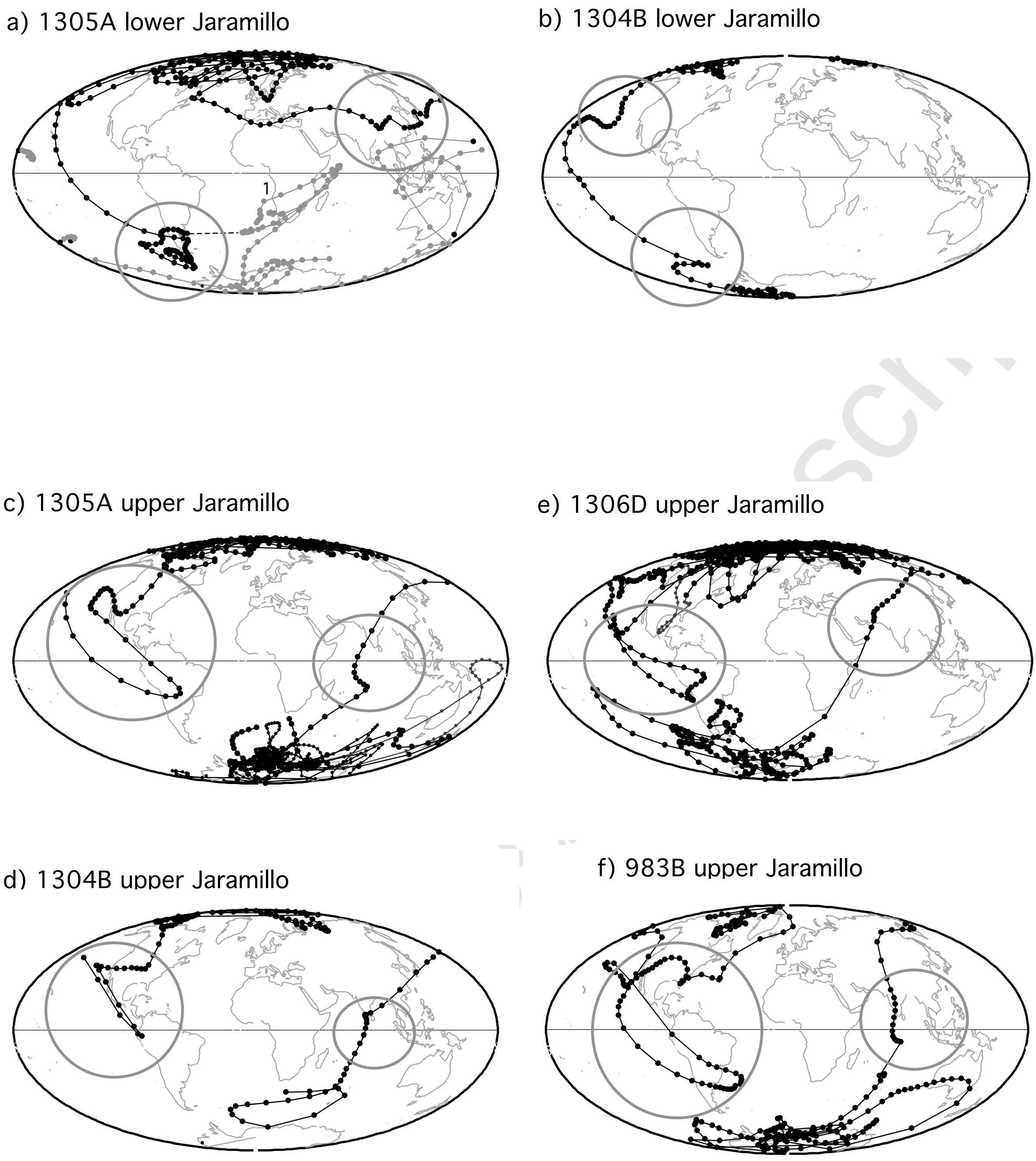
a) 1305A lower Jaramillo
1
b) 1304B lower Jaramillo
c) 1305A upper Jaramillo
e) 1306D upper Jaramillo
d) 1304B upper Jaramillo
f) 983B upper Jaramillo